

Avalanches at rough surfaces

G. C. Barker*

Institute of Food Research, Norwich Research Park, Colney, Norwich NR4 7UA, United Kingdom

Anita Mehta†

S. N. Bose National Centre for Basic Sciences, Block JD, Sector III, Salt Lake, Calcutta 700091, India

(Received 4 October 1999)

We describe the surface properties of a simple lattice model of a sandpile that includes evolving structural disorder. We present a dynamical scaling hypothesis for generic sandpile automata and, additionally, explore the kinetic roughening of the sandpile surface, indicating its relationship with the sandpile evolution. Finally, we comment on the surprisingly good agreement found between this model, and a previous continuum model of sandpile dynamics, from the viewpoint of critical phenomena.

PACS number(s): 45.70.-n, 05.50.+q, 81.05.Rm

INTRODUCTION

Avalanches are the signatures of instabilities on an evolving surface: regions on a sandpile, for example, which protrude excessively from the surface, get dislodged by such mechanisms. This most intuitive picture of avalanching [1,2] is the one we seek to model and study: although presented here in the context of sandpiles, a similar picture may be relevant to intermittent granular flows along an inclined plane [3], or to sediment consolidation [4]. As deposition occurs on a sandpile surface, clusters of grains grow unevenly at different positions and roughness builds up until further deposition renders some of the clusters unstable. These then start toppling, so that grains from an already unstable cluster flow down the sandpile, knocking off grains from other similar clusters which they encounter. The net effect of this is to wipe off protrusions (where there is a surfeit of grains at a cluster) and to fill in dips, where the oncoming avalanche can disburse some of its grains. In short, the surface is smoothed by the passage of the avalanche so that there is a rough precursor surface, and a smoothed post-avalanche surface.

In earlier work [5,6], we explored this issue via an analytical model involving coupled continuum equations. Here we use a cellular-automaton (CA) model [7] of an evolving sandpile to look in more depth at the mechanisms by which a large avalanche smooths the surface. Our sandpile model is a disordered and non-Abelian version of the basic Kadanoff cellular automaton [8]; a further degree of freedom, which involves granular reorganization within columns, is added to the basic model, which includes only granular flow between columns. In this sense, each column is regarded as a cluster of grains so that we represent intracluster as well as intercluster grain relaxations, in accord with a previous understanding of sandpile dynamics [9].

Our disordered model sandpile [10] is built from rectangular lattice grains, that have aspect ratio $a \leq 1$ arranged in columns i with $1 \leq i \leq L$, where L is the system size. Each

grain is labeled by its column index i and by an orientational index 0 or 1, corresponding, respectively, to whether the grain rests on its larger or smaller edge.

The dynamics of our model have been described at length elsewhere [7] but we review the essentials here.

(1) Grains are deposited on the sandpile with fixed probabilities of landing in the 0 or 1 position.

(2) The incoming grains, as well as all the grains in the same column, can then “flip” to the other orientation stochastically (with probabilities that decrease with depth from the surface). This flip, or change of orientation, is our simple representation of *collective dynamics in granular clusters*, since typically clusters reorganize owing to the slight orientational movements of the grains within them [9].

(3) Column heights are then computed as follows. The height of column i at time t , $h(i,t)$, can be expressed in terms of the instantaneous numbers of 0 and 1 grains, $n_0(i,t)$ and $n_1(i,t)$, respectively:

$$h(i,t) = n_1(i,t) + an_0(i,t). \quad (1)$$

(4) Finally, grains fall to the next column down the sandpile (maintaining their orientation as they do so) if the height difference exceeds a specified threshold in the normal way [8] (the pile is local, limited, and has a fall number of two). At this point, avalanching occurs.

In earlier papers, [7], it was shown that the presence of disorder led, for large enough system sizes, to a preferred size of large avalanches. In the absence of disorder, scale-invariant avalanche statistics were observed. In this work, we focus on the state of the sandpile surface [11] in a bid to correlate its evolution with the onset and propagation of avalanches.

I. DYNAMICAL SCALING FOR SANDPILE CELLULAR AUTOMATA

It is customary in the study of generalized surfaces to examine the widths generated by kinetic roughening [12] and then establish properties related to *dynamical scaling*. However, the kinetic roughening of sandpile cellular automata has never been investigated; to begin with, therefore, we pos-

*Electronic address: barker@bbsrc.ac.uk

†Electronic address: anita@boson.bose.res.in

tulate a principle of *dynamical scaling for sandpile cellular automata* in terms of the surface width W of the sandpile automaton:

$$W(t) \sim t^\beta, t \leq t_{\text{crossover}} \equiv L^z, \quad (2)$$

$$W(L) \sim L^\alpha, L \rightarrow \infty. \quad (3)$$

As in the case of interfacial widths, these equations signify the following sequence of roughening regimes.

(1) To start with, roughening occurs at the CA sandpile surface in a time-dependent way; after an initial transient, the width scales asymptotically with time t as t^β , where β is the *temporal roughening* exponent. This regime is appropriate for all times less than the crossover time $t_{\text{crossover}} \equiv L^z$, where $z = \alpha/\beta$ is the dynamical exponent and L the system size.

(2) After the surface has *saturated*, i.e., its width no longer grows with time, the *spatial roughening* characteristics of the mature interface can be measured in terms of α , an exponent characterizing the dependence of the width on L .

We define the surface width $W(t)$ for a sandpile automaton in terms of the mean-squared deviations from a suitably defined mean surface; in analogy with the conventional counterpart for interface growth [12], we define the instantaneous mean surface of a sandpile automaton as the surface about which the sum of column *height* fluctuations vanishes. Clearly, in an evolving surface, this must be a function of time; hence all quantities in the following analysis will be presumed to be instantaneous.

The mean slope $\langle s(t) \rangle$ defines expected column heights, $h_{av}(i, t)$, according to

$$h_{av}(i, t) = i \langle s(t) \rangle, \quad (4)$$

where we have assumed that column 1 is at the bottom of the pile. Column height deviations are defined by

$$dh(i, t) = h(i, t) - h_{av}(i, t) = h(i, t) - i \langle s(t) \rangle. \quad (5)$$

The mean slope must therefore satisfy

$$\sum_i [h(i, t) - i \langle s(t) \rangle] = 0, \quad (6)$$

since the instantaneous deviations about it vanish; thus

$$\langle s(t) \rangle = 2 \sum_i [h(i, t)] / L(L+1). \quad (7)$$

(We note that this slope is distinct from the quantity $\langle s'(t) \rangle = h(L, t) / L$ that is obtained from the average of all the local slopes $s(i, t) = h(i, t) - h(i-1, t)$, about which *slope* fluctuations would vanish on average).

The instantaneous width of the surface of a sandpile automaton, $W(t)$, can be defined as

$$W(t) = \sqrt{\sum_i [dh(i, t)^2]} / L, \quad (8)$$

which can in turn be averaged over several realizations to give, $\langle W \rangle$, the average surface width in the steady state.

We also compute here the height-height correlation function, $C(j, t)$, which is defined by

$$C(j, t) = \langle dh(i, t) dh(i+j, t) \rangle / \langle dh(i, t)^2 \rangle, \quad (9)$$

where the mean values are evaluated over all pairs of surface sites separated by j lattice spacings:

$$\langle dh(i, t) dh(i+j, t) \rangle = \sum_i [dh(i, t) dh(i+j, t)] / (L-j) \quad (10)$$

for $0 \leq j < L$. This function is symmetric and can be averaged over several realizations to give the average correlation function $\langle C(j) \rangle$.

II. QUALITATIVE EFFECTS OF AVALANCHING ON SURFACES

Before moving on to the quantitative descriptors of sandpile avalanching and surface roughening, we present some results using more qualitative indicators. Recent experiments [3] on sandpile avalanches have indicated that there are at least two broad categories; uphill avalanches, which are typically large, and triangular avalanches, which are generally smaller in size. We have found evidence of this in a $(2+1)$ -dimensional disordered model of sandpile avalanches, which will be presented elsewhere [13]; but in this work we discuss analogues in $(1+1)$ dimension, which are, respectively, wedge-shaped and flat avalanches. The following data indicate that it is the larger wedge-shaped avalanches that alter surface slope and width, while the flatter, smaller avalanches alter neither one very much. This is in accord with earlier work, where it was found that larger avalanches are the consequence of accumulated disorder, while the smaller ones can cause disordered regions to build up along the sandpile surface [14].

Figure 1(a) shows a time series for the mass of a large ($L=256$) evolving disordered sandpile automaton. The series has a typical quasiperiodicity [1]. The vertical line denotes the position of a particular large event, while Fig. 1(b) shows the avalanche size distribution for the sandpile. Note the peak, corresponding to the preferred large avalanches, which was analyzed extensively in earlier work [7]. Our data show that the avalanche highlighted in Fig. 1(a) drained off approximately 5% of the mass of the sandpile, placing it close to the second peak of Fig. 1(b). Figure 1(c) shows the outline of the full avalanche before and after this event with its initiation site marked by an arrow; we note that, as is often the case in one dimension, the avalanche is uphill. The inset shows the relative motion of the surface during this event; we note that the signatures of smoothing by avalanches are already evident, since the precursor state in the inset is much rougher than the final state. Finally we show in Fig. 1(d) the grain-by-grain picture of the aftermath pile superposed on the precursor pile, which is shown in shadow. An examination of the aftermath pile and the precursor pile shows that the propagation of the avalanche across the upper half of the pile has left only a very few disordered sites in its wake (i.e., the majority of the remaining sites are 0 type), whereas the lower half (which was undisturbed by the avalanche) still contains many disordered, i.e., 1-type sites in the boundary layer. This leads us to suggest that the larger avalanches rid the boundary layer of its disorder-induced roughness, a fact that is borne out by our more quantitative investigations.

In fact, our studies have revealed that the very largest avalanches, which are system-spanning, remove virtually all

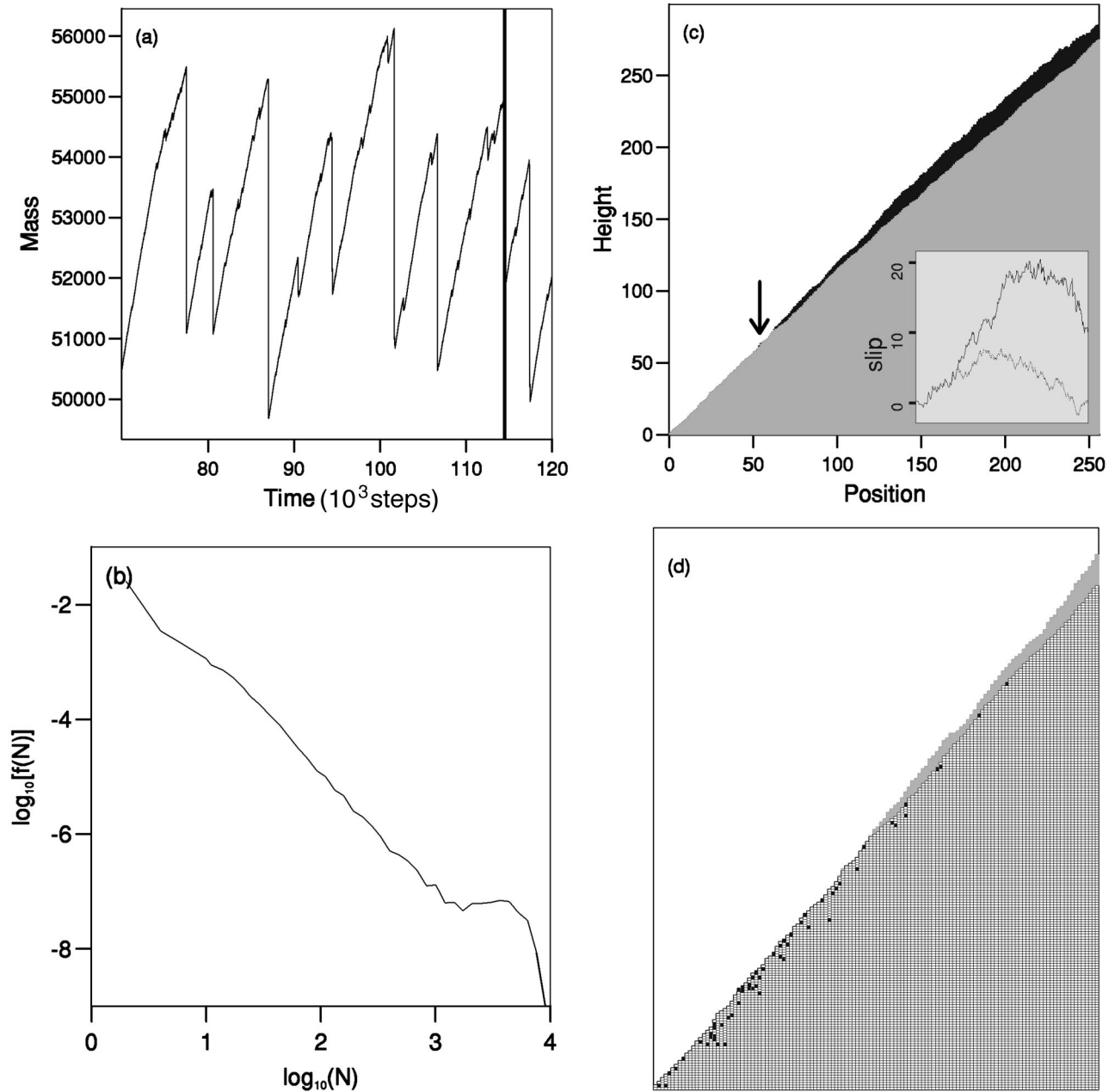


FIG. 1. (a) A time series of the mass for a model sandpile ($L=256$) that has been built to include a surface layer containing structural disorder (mass is measured in lattice grain units). The vertical line indicates the position in this series of the large avalanche illustrated in Figs. 1(c) and 1(d). (b) A log-log plot of the event size distribution for a model sandpile ($L=256$) that includes a surface layer containing structural disorder. (c) An illustration of a large wedge-shaped avalanche in a model sandpile ($L=256$) that has been built to include a surface layer containing structural disorder. A lighter aftermath pile has been superposed onto the dark precursor pile and an arrow shows the point at which the event was initiated. The inset shows the relative positions of the two surfaces and their relationship to a pile that has a smooth slope (height and position are measured in lattice units). (d) A detailed picture of the internal structure of a model sandpile in the aftermath of a large avalanche event. The individual grains of the aftermath pile (for columns 1–128 of a sandpile with $L=256$) are superposed on the gray outline of the precursor pile.

disordered sites from the surface layer; one is then left with a normal ordered sandpile, where the avalanches have their usual scaling form for as long as it takes for a layer of disorder to build up. When the disordered layer reaches a critical size, another large event is unleashed; this is the underlying reason for the quasiperiodic form of the time series shown in Fig. 1(a).

Before moving on to more quantitative features, we show for comparison the sequence of Fig. 1, for (1) an ordered pile

[Figs 2(a)–2(d)]; (2) a small disordered pile [Figs. 3(a)–3(d)]

We note the following features.

(1) The small disordered pile has a mass time series [Fig. 3(a)] that is midway between the scale invariance of the ordered pile [Fig. 2(a)] and the quasiperiodicity of the large disordered pile [Fig. 1(a)].

(2) The avalanche size distribution of the small disordered pile [Fig. 3(b)] is likewise intermediate between that of the

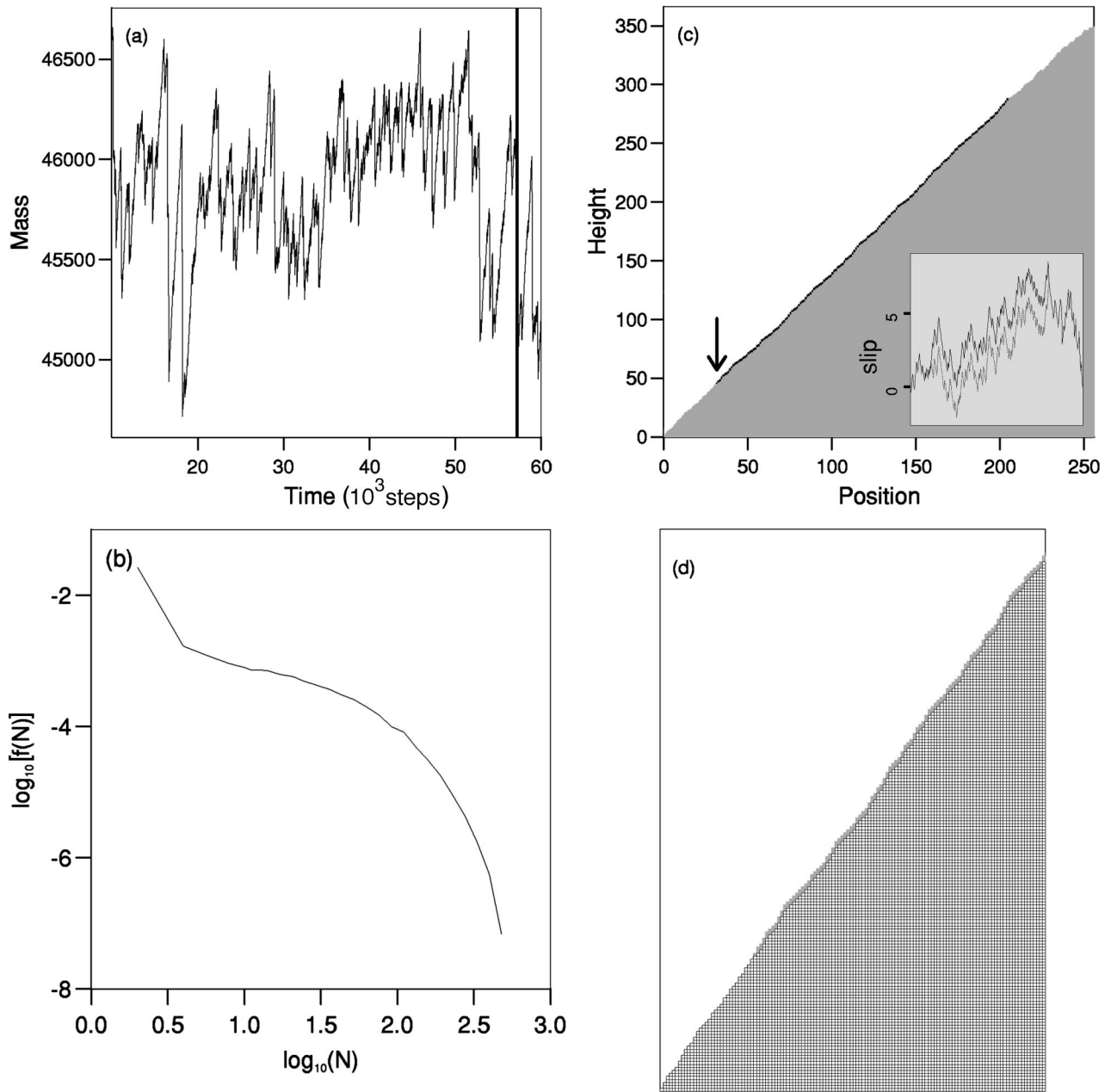


FIG. 2. (a) A time series of the mass for a model sandpile ($L=256$) that has been built to exclude any structural disorder (mass is measured in lattice grain units). The vertical line indicates the position in the series of the avalanche illustrated in Figs. 2(c) and 2(d). (b) A log-log plot of the event size distribution for a model sandpile ($L=256$) that excludes structural disorder. (c) An illustration of a large flat avalanche in a model sandpile ($L=256$) that excludes structural disorder. A lighter aftermath pile has been superposed onto the dark precursor pile and an arrow shows the point at which the event was initiated. The inset shows the relative positions of the two surfaces and their relationship to a pile that has a single smooth slope (height and position are measured in lattice units). (d) A detailed picture of the internal structure of a model sandpile in the aftermath of a large avalanche event. The individual grains for the aftermath pile (for columns 1 – 128 of an ordered pile with $L=256$) are superposed on the grey outline of the precursor pile.

ordered pile (which shows the scale invariance observed by Kadanoff *et al.* [8]) and the two-peaked distribution characteristic of the disordered pile [7].

(3) In both small and large disordered piles, we see evidence of large uphill avalanches that shave off a thick boundary layer containing large numbers of disordered sites, and leave behind a largely ordered pile [see Figs. 1(c) and 1(d) and Figs 3(c) and 3(d)]. By contrast, the ordered pile loses typically two commensurate layers even in the largest

avalanche, with a correspondingly unexciting aftermath state left behind in its wake [Figs. 2(c) and 2(d)].

We conclude from this that there is, even at a qualitative level, a post-avalanche smoothing of the sandpile surface, beyond a crossover length, as found in earlier work on continuum models [5]; importantly, our discrete model reveals that this is achieved by the removal of (orientational) disorder, the implications of which we will discuss in our concluding section. The existence of the crossover length, in

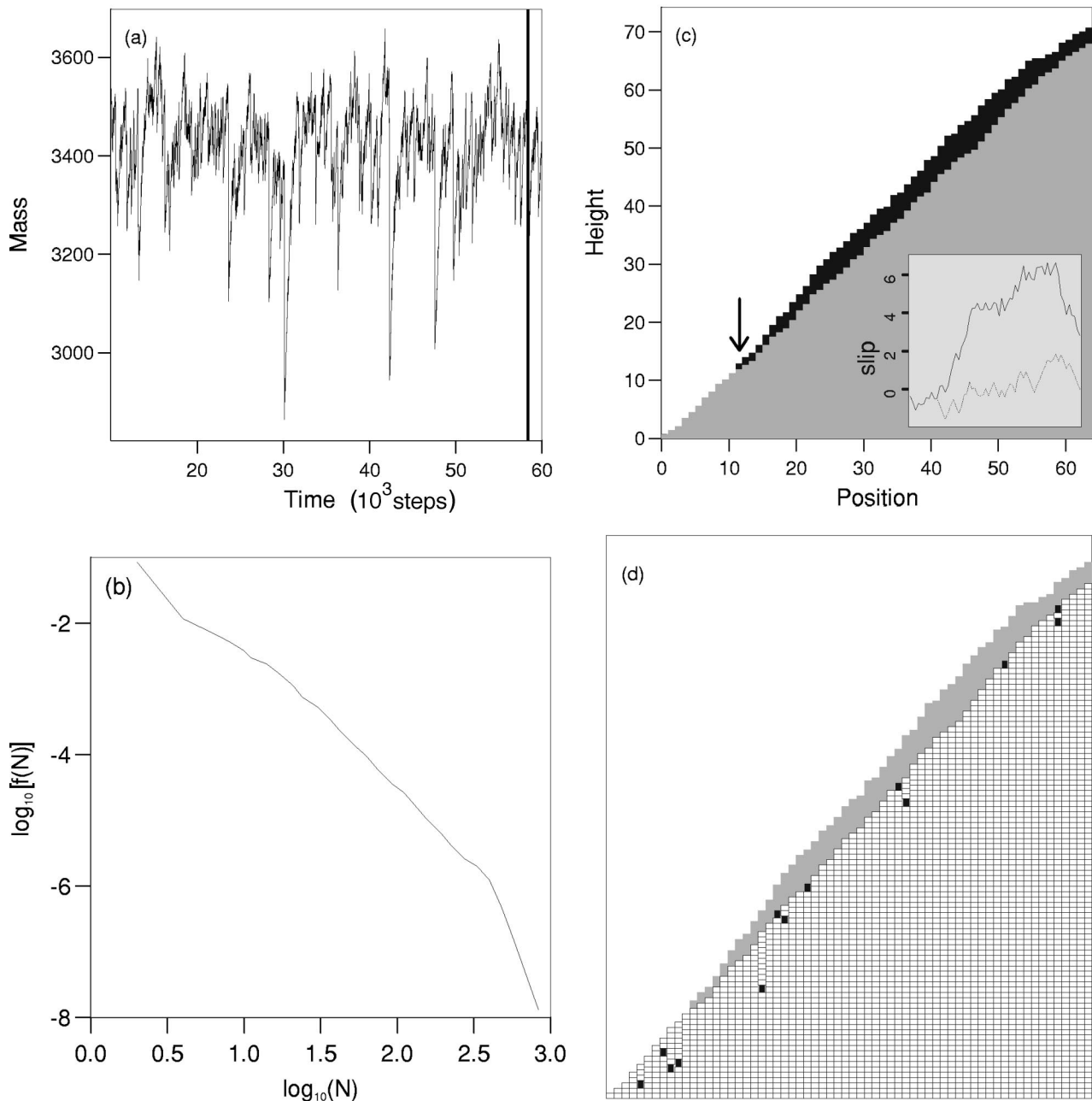


FIG. 3. (a) A time series of the mass for a model sandpile ($L=64$) that has been built to include a surface layer containing structural disorder (mass is measured in lattice grain units). The vertical line indicates the position in this series of the large avalanche illustrated in Figs. 3(c) and 3(d). (b) A log-log plot of the event size distribution for a model sandpile ($L=64$) that includes a surface layer containing structural disorder. (c) An illustration of a large wedge-shaped avalanche in a model sandpile ($L=64$) that has been built to include a surface layer containing structural disorder. A lighter aftermath pile has been superposed onto the dark precursor pile and an arrow shows the point at which the event was initiated. The inset shows the relative positions of the two surfaces and their relationship to a pile that has a smooth slope (height and position are measured in lattice units). (d) A detailed picture of the internal structure of a model sandpile in the aftermath of a large avalanche event. The individual grains of the aftermath pile are superposed on the gray outline of the precursor pile.

terms of the mass time series, has also been observed in experiment [1].

III. QUANTITATIVE EFFECTS OF AVALANCHING ON SURFACES

A. Intrinsic properties of sandpile surfaces

Inspired by the picture of smoothing avalanches, we have investigated many of the material properties of the sandpile

in the special pre- and post-avalanche configurations. From these we have drawn the following conclusions.

(1) The *mean slope* of the disordered sandpile peaks (see Table I) before a large avalanche and drops immediately after; this statement is true for events of any size and thus remains trivially true for the ordered sandpile.

(2) The *packing fraction* ϕ of the disordered sandpile increases after a large event, i.e., effective consolidation occurs during avalanching (see Table I). This consolidation via

TABLE I. Instantaneous properties of disordered model sandpiles.

L	State of pile	Packing fraction ϕ	Slope	Width
256	before	0.997	1.15	4.45
256	after	1.000	1.07	2.06
64	before	0.991	1.17	1.41
64	after	0.998	1.04	1.15

avalanching mirrors that which occurs when a sandpile is shaken with low-intensity vibrations [15,16].

(3) However, a far more significant statement can be made about the comparison of the surface width for pre- and post-large-event sandpiles; Table I shows that the surface width shrinks considerably during an event, once again suggesting that a rough precursor pile is smoothed by the propagation of a large avalanche.

We have also investigated the dependence of various material properties of a disordered sandpile on the aspect ratio of the grains [17]. Table II shows our results, and Fig. 4 illustrates the variation of the avalanche size distribution.

There is a transition as aspect ratios of 0.7 are approached from above or below; we have shown above that piles with these critical aspect ratios manifest strong disorder [7] in the sense of (a) a second peak in the avalanche size distribution denoting a preferred size of large avalanches; (b) large surface widths denoting an increased surface roughness; (c) a strong correlation between interfacial roughness and avalanche flow, since the mean surface width varies dramatically in the pre- and post-large-event piles.

Clearly, sandpiles containing grains with aspect ratios close to unity act essentially as totally ordered piles [8]; there is, however, a significant symmetry in the shape of the avalanche size distribution curves above and below the transition region [see Figs. 4(a) and 4(d)]. These size distributions are reminiscent of those obtained in earlier work [7] for the case of uniform disorder (which referred to piles that have disorder throughout their volume rather than, as is the present case, disorder concentrated in a boundary layer). These observations lead us to speculate that there exist at least three types of avalanche spectra:

(1) the scale-invariant statistics characteristic of ordered sandpiles;

(2) the strongly disordered statistics characterized by a second peak in the distribution, which we have obtained for specific values of the aspect ratio in the case where the dis-

TABLE II. Properties of model sandpiles.

Aspect ratio	Packing fraction ϕ	Slope	Width
0.6	0.997	1.44	2.33
0.65	0.997	1.42	2.34
0.7	0.997	1.12	3.76
0.75	0.997	1.19	3.74
0.8	0.998	1.17	2.35
0.9	0.999	1.25	2.29
0.95	1.000	1.32	2.37
1.0	1.000	1.40	2.41

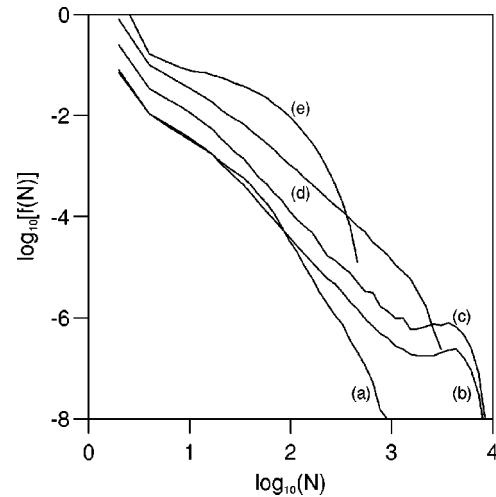


FIG. 4. Exit mass event size distributions for a disordered sandpile model with $L=256$, and $a=$ (a) 0.6, (b) 0.7, (c) 0.75, (d) 0.85, (e) 1.0. The curves have each been shifted by 0.5 to make them distinct.

order is concentrated in a boundary layer;

(3) the more weakly disordered region (characterized by a flatter size distribution of avalanche sizes which is, nevertheless, *not* scale invariant) obtained in the intermediate regimes of aspect ratio (as well as in the case of uniform disorder).

It is clear that *the presence of inherent inhomogeneities in grain shape (which we describe quantitatively by aspect ratio) or bulk structure (which we describe by the classifications of uniform or boundary disorder) in a sandpile induces the presence of strong disorder in avalanche statistics.*

Additionally, we present, in Fig. 5, the mass-mass correlation function of a particular disordered sandpile; the curve has a peak, which indicates the average time between avalanches. Since the avalanche size distribution for this sandpile includes a preponderance of large events, we conclude that the peak in the correlation function corresponds approximately to the *time between large avalanches*. We also expect this time scale to manifest itself in the power spectrum of the avalanches; and we expect it to vary strongly with the level and nature of disorder in the sandpile. This work is in progress, as are efforts to relate the time scale found above to

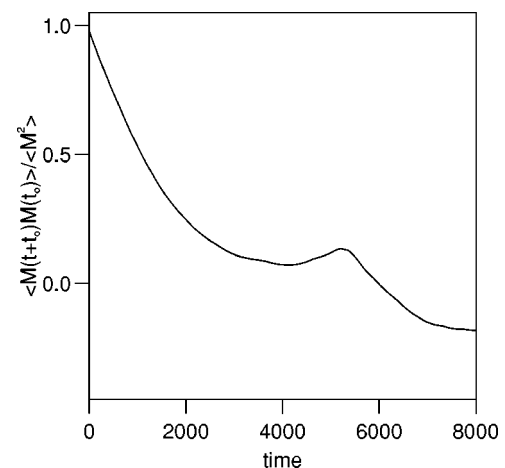


FIG. 5. The mass-mass correlation function for a disordered model sandpile with $L=256$.

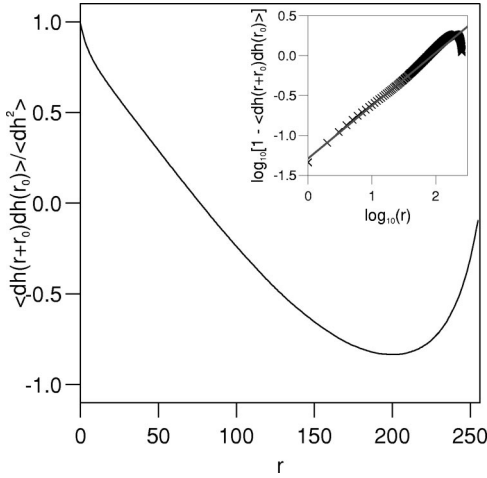


FIG. 6. The normalized correlation function of column height deviations for a disordered model sandpile with $L=256$. The inset illustrates an initial decay with r , going as $r^{-0.67}$ (r is measured in lattice units).

a characteristic spatial signature for large events.

We present in Fig. 6 the normalized *equal-time* height-height correlation function $\langle dh(r+r_0)dh(r_0) \rangle / \langle dh_0^2 \rangle$ for a disordered sandpile. This shows that the height deviations (from the instantaneous expected column heights), in a disordered sandpile with $L=256$, are positively correlated over about 80 columns, but also have a range where they are negatively correlated. In the inset we plot the related function $1 - \langle dh(r+r_0)dh(r_0) \rangle / \langle dh_0^2 \rangle \equiv [dh(r+r_0) - dh(r_0)]^2 / 2\langle dh_0^2 \rangle$. For separations r much less than the correlation length of the system, we should have [18]

$$\langle [dh(r+r_0) - dh(r_0)]^2 \rangle \sim |r|^{2\alpha} \quad (11)$$

and, therefore, we would expect the function in the inset of Fig. 6 to manifest a similar r dependence. A linear fit to points with $r < 30$ (shown by the line in the inset of Fig. 6) indicates a power-law dependence of the form $r^{0.67}$ for $r \ll L$, implying that $\alpha \sim 0.34$. As we will see below, this corresponds to the spatial roughening exponent of an *ordered* sandpile. An explanation of this behavior is included in the next section.

B. Spatial and temporal roughening of sandpile surfaces

The hypothesis of dynamical scaling for sandpiles assumes that the roughening process occurs in two stages. First, the surface roughening is time dependent, Eq. (2); then once the roughness becomes temporally constant, the surface is said to saturate, and all further deposition results in surface fluctuations governed by Eq. (3).

However, there is a subtlety concerning the first (i.e., time-dependent) stage; early model sandpiles are wedge shaped and the transition to saturation is accompanied by a gradual buildup to a pile that has a single, sloping surface with a suitable angle of repose.

We have taken this process into account to measure the dynamic exponent β , Eq. (2); in this case surface widths are evaluated from the sloping portion of the pile. For the roughening exponent α , Eq. (3), we have measured surface widths from mature piles that have only a sloping surface.

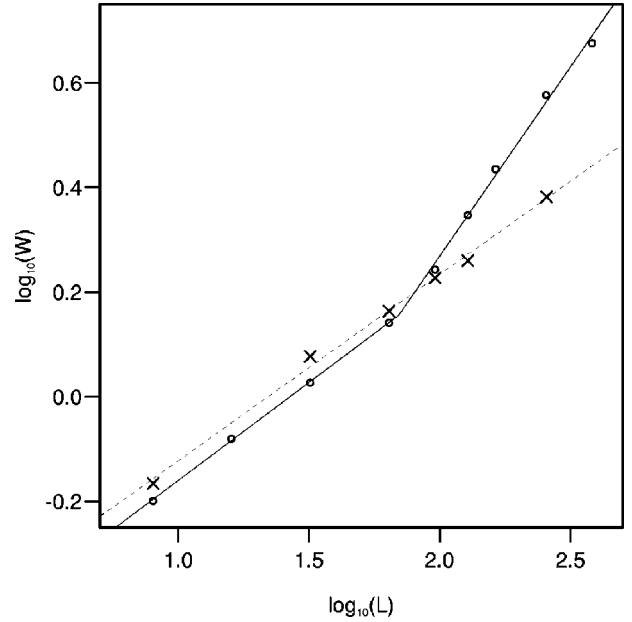


FIG. 7. A log-log plot of the surface widths W against the system size L for model sandpiles; \times , ordered piles; \circ , disordered piles. Widths are measured in lattice units and all points have error bars that are ~ 0.02 .

Our results are as follows.

- For disordered sandpiles ($L=2048$) we find $\beta=0.42 \pm 0.05$; for ordered sandpiles ($L=2048$), $\beta=0.17 \pm 0.05$.
- For disordered sandpiles above a crossover size of $L_c=90$ we find $\alpha=0.723 \pm 0.04$, while for ordered piles we find $\alpha=0.356 \pm 0.05$.
- Based on the above values, we find the dynamical exponent z has values of 1.72 ± 0.29 and 2.09 ± 0.84 for the disordered and ordered sandpiles, respectively.

The variation of the surface width W as a function of L is shown in a log-log plot in Fig. 7. This figure shows clearly the crossover in α as a function of system size, for disordered sandpiles; the scaling behavior of ordered sandpiles is shown for comparison. Disordered sandpiles with sizes below L_c have $\alpha=0.37 \pm 0.05$; this is in accord with earlier work [7], where the second peak in the avalanche spectrum appeared only for disordered piles above crossover. The existence of this crossover length has been variously interpreted as a length related to reorganization in the boundary layer of a sandpile [9] or to variations in the angle of repose in a (disordered) sandpile [19]. Disorder appears to be crucial for the existence of such experimentally observed crossovers, since, for example, ordered models [20,21] show no crossover in their measurements of α . The crossover effect in a disordered sandpile is also indicated by the height-height correlation function (Fig. 6). For separations $r \ll L_c \sim 90$ in disordered sandpiles (with length $L \gg L_c$), the exponent α obtained from the small r behavior of the correlation function is that of the ordered sandpile. This suggests that even in disordered sandpiles, grains that are within a crossover length L_c of each other tend to order, i.e., examination of the height-height correlation function for separations $r \ll L_c$ (Fig. 6) or direct measurement of α for system sizes $L \ll L_c$, as reported above, yields the exponent of the ordered sandpile, $\alpha \sim 0.35$.

The above values indicate that while there is no change of universality class as one goes from an ordered to a disordered sandpile (z stays the same, within the error bars), the disordered pile is clearly rougher with respect to both temporal and spatial fluctuations (α and β higher).

It is important to note that our measurements of surface exponents are taken over many realizations of the surfaces concerned. Thus, even though, as demonstrated in earlier sections, the surface of a disordered sandpile is temporarily smoothed by the propagation of a large avalanche, it begins to roughen again as a result of deposition; the values of α and β that we measure are averages over millions of such cycles and hence reflect the roughening of the interface, in an average sense. By contrast, no abnormally large events occur for the ordered sandpiles and this is reflected by the lower values of fluctuations and exponents.

The most striking aspect of these exponents is that they indicate that our present cellular-automaton model is a discrete version of earlier continuum equations [5], which were formulated independently, to model the pouring of grains onto a sloping surface. The exponents for our disordered pile are within error bars, exactly those that were measured for the height fluctuations of the surface in case 2, of Ref. [5], while those for the ordered pile are exactly those that were measured for the fluctuations of the avalanches generated by the mobile grains in the same case. This is in accord with the notion that the avalanches that flow on an ordered pile generate only mobile grains on the otherwise ordered surface, while as we have demonstrated above, avalanches that flow on a disordered pile, also *change the configuration of the surface* by altering the distribution of height fluctuations

(measured by the surface widths). We are exploring these analogies further, but note that this agreement is already a strong validation of both models.

IV. DISCUSSION AND CONCLUSIONS

We have presented a thorough investigation of the effects of avalanching on a sandpile surface, focusing on the inter-relationship between the nature of the avalanches and the surfaces they leave behind. We have also postulated a principle of dynamical scaling for sandpile surfaces, and measured the roughening exponents for a sample disordered sandpile. Finally, we have related the characteristics of avalanching in our model system to those obtained experimentally.

Our current investigations concern several questions left unanswered above. These include the dependence of the crossover length L_c on the disorder in the pile; as well as a fuller investigation of the effect of the nature of disorder (i.e., whether boundary or uniform). We would expect our correlation functions to depend strongly on the nature and magnitude of the disorder and we are undertaking a full quantitative study. Last, we hope that an extension of the present analysis to higher dimensions will yield more extensive comparisons with experiments than are presently available.

ACKNOWLEDGMENT

G.C.B. acknowledges support from the Biotechnology and Biological Sciences Research Council, UK (Grant No. 218/FO6522).

-
- [1] H.M. Jaeger, C. Liu, and S.R. Nagel, Phys. Rev. Lett. **62**, 40 (1989); G.A. Held, D.H. Solina, D.T. Keane, W.J. Haag, P.M. Horn, and G. Grinstein, *ibid.* **65**, 1120 (1990).
 - [2] H.M. Jaeger, S.R. Nagel, and R.P. Behringer, Rev. Mod. Phys. **68**, 1259 (1996).
 - [3] Adrien Daerr and Stéphane Douady, Nature (London) **399**, 241 (1999).
 - [4] R.E. Snyder and R.C. Ball, Phys. Rev. E **49**, 104 (1994).
 - [5] Anita Mehta, J.M. Luck, and R.J. Needs, Phys. Rev. E **53**, 92 (1996).
 - [6] P. Biswas, A. Majumdar, Anita Mehta, and J.K. Bhattacharjee, Phys. Rev. E **58**, 1266 (1998).
 - [7] Anita Mehta and G.C. Barker, Europhys. Lett. **27**, 501 (1994); Anita Mehta, G.C. Barker, J.M. Luck, and R.J. Needs, Physica A **224**, 48 (1996).
 - [8] L.P. Kadanoff, S.R. Nagel, L. Wu, and S-M Zhou, Phys. Rev. A **39**, 6524 (1989); P. Bak, C. Tang, and K. Wiesenfeld, *ibid.* **38**, 364 (1988).
 - [9] Anita Mehta, Physica A **186**, 121 (1992); Anita Mehta, in *Granular Matter: An Interdisciplinary Approach*, edited by Anita Mehta (Springer-Verlag, New York, 1994).
 - [10] Throughout this paper we refer to disordered sandpiles described in reference [7] with parameters $z_0=2$, $z_1=20$, and $a=0.7$, unless otherwise stated.
 - [11] Anita Mehta in *Structure and Dynamics of Materials in the Mesoscopic Domain*, edited by M. Lal *et al.* (Imperial College Press and the Royal Society, London, 1999), p. 340.
 - [12] J. Krug, Adv. Phys. **46**, 1 (1997).
 - [13] G.C. Barker and Anita Mehta, Physica A (to be published).
 - [14] G.C. Barker and Anita Mehta, Phys. Rev. E **53**, 5704 (1996).
 - [15] Anita Mehta and G.C. Barker, Phys. Rev. Lett. **67**, 394 (1991).
 - [16] J.B. Knight, C.G. Fandrich, C.N. Lau, H.M. Jaeger, and S.R. Nagel, Phys. Rev. E **51**, 3957 (1995); E.R. Nowak, J.B. Knight, E. Ben-Naim, H.M. Jaeger, and S.R. Nagel, *ibid.* **57**, 1971 (1998).
 - [17] V. Frette, K. Christensen, A. Malthe-Sorensen, J. Feder, T. Jossang, and P. Meakin, Nature (London) **379**, 49 (1996).
 - [18] L. Sander, in *Solids Far From Equilibrium*, edited by C. Godrèche (Cambridge University Press, Cambridge, 1991).
 - [19] S.R. Nagel, Rev. Mod. Phys. **64**, 321 (1992).
 - [20] M. Paczuski and S. Boettcher, Phys. Rev. Lett. **77**, 111 (1996).
 - [21] T. Hwa and M. Kardar, Phys. Rev. A **45**, 7002 (1992).